Extreme ultraviolet photoemission of transition-metal chlorides excited with synchrotron radiation*

T. Ishii, S. Kono, S. Suzuki, and I. Nagakura†
Department of Physics, Tohoku University, Sendai, Japan

T. Sagawa,‡ R. Kato,§ M. Watanabe, and S. Sato
Institute for Solid State Physics, University of Tokyo, Roppongi, Tokyo, Japan
(Received 28 April 1975)

Synchrotron radiation monochromatized at energies 76, 61, and 40 eV has been used to obtain the photoemission spectra of valence electrons in $NiCl_2$, $CoCl_2$, $FeCl_2$, and $MnCl_2$. Only slight dependence of the spectra on excitation energy is found for three excitation energies employed here. Although the observed gross features of the spectra are consistent with the x-ray photoelectron spectra of these materials, the profiles of the spectra are partly different from those of the x-ray photoelectron spectra. The contribution of the $3p$ electrons of Cl^- ions to the photoelectron spectra relative to those of the $3d$ electrons of transition-metal ions may be different between extreme ultraviolet and x-ray excitations. Detailed comparison with the x-ray photoelectron spectra has been made to separate the components arising from the $3d$ electrons of transition-metals ions. Their line shapes are in good agreement with the spectral distributions of the multiplet levels of the $3d$ electrons in the final states derived from a simple ligand-field treatment.

I. INTRODUCTION

Energy-band theory is known to be quite useful to treat the electronic energy states of crystalline solids such as metals and semiconductors. It is also known that the energy-band picture often fails to explain the phenomena related to the optical excited states of solids like exciton absorption in insulators[1] and Fermi-edge anomalies in soft-x-ray absorption or emission in light metals.[2] There are a group of solids for which the itinerant-electron model as in energy-band theory is inadequate even in the ground state.[3] Transition-metal chlorides belong to this kind of materials. The presence of unfilled localized $3d$ shells has a significant influence on the electronic properties of these materials. Both the $3d$ electrons of transition-metal ions and the $3p$ electrons of chlorine contribute to the valence state. In a case like this, the molecular-orbital approach is suitable for interpreting optical-absorption data, if the electron-correlation effect in the final state is appropriately taken into account. As in the case of ligand-field theory,[4] energy levels are characterized by the symmetry property of a molecular unit interacting with photons.

Photoelectron spectroscopy is an ingenious method to investigate the energy states of valence electrons as well as core electrons. X-ray photoelectron spectroscopy (XPS) usually employs radiation of 1.25 keV (Mg $K\alpha$) or 1.48 keV (Al $K\alpha$) for exciting photoelectrons. Observed valence-state spectra reflect the density of states or, more rigorously, the partial density of states modified by the transition moment. In ultraviolet photoelectron spectroscopy (UPS), where exciting radiation has energies less than 30 eV, valence-state spectra are greatly modified by the conservation of the electron wave vector. Extreme-ultraviolet photoelectron spectroscopy (EUPS) is more like XPS. Radiation below 100 eV is easily monochromatized with better resolution to give the better over-all resolution of the photoelectron spectrum than the XPS case. The modification due to the energy or wave-vector dependence of the transition moment is not important in narrow spectral regions to be observed. The difference in the transition moment between valence electrons with different orbital angular momenta should be taken into account in the analysis of the valence-state spectrum. The dependence of the transition moment on excitation energy becomes important in the comparison of EUPS spectra with XPS or UPS spectra. Powerful extreme-ultraviolet radiation with continuous spectrum is provided by an electron synchrotron or an electron storage ring.

The purpose of this paper is to present the EUPS spectra of valence electrons in the chlorides of nickel, cobalt, iron, and manganese, obtained by excitation with monochromatized synchrotron radiation. The spectra will be interpreted on the basis of the energy levels of the $3d$ electrons of transition-metal ions.

II. EXPERIMENTAL

The schematic illustration of the experimental arrangement has been given elsewhere.[5] Synchrotron radiation from a 1.3-GeV electron synchrotron at the Institute for Nuclear Study, University of Tokyo, was monochromatized with an optical system consisting of a plane mirror, a toroidal mirror, and a concave grating. Monochromatized radiation was focused on the sample surface as a small spot. All optical elements were placed so that radiation was dispersed in a vertical plane. No slit was used in the optical system. The mono-

chromator was not equipped with any driving systems for changing the wavelength of monochromatized radiation; every time the wavelength was changed, the mirrors and the grating were remounted to get new positions and incident angles. Excitation energies employed here were 40, 61, and 76 eV.

Samples were prepared by evaporation in a separate sample chamber and transported into the analyzer chamber without breaking vacuum. The substrate made of a copper rod was heated at about 150 °C during the evaporation and kept at this temperature for several minutes after the evaporation. Such a heat treatment is known to be important to obtain a good sample.[6] The pressure in the analyzer chamber during the measurements was about 5×10^{-9} Torr.

An electron-energy analyzer of a two-stage cylindrical-mirror type was used to measure the energy distribution of photoelectrons. Radiation from the electron synchrotron was pulsed with a repetition rate of 21.5 Hz, and its intensity fluctuated from time to time. Thus, the intensity of incident radiation was monitored at the entrance to permalloy cases for magnetic shielding, and the monitor signal was used to drive the voltage supply to the analyzer electrodes. The over-all resolution of the photoelectron spectrometer used here was estimated to be 0.5 eV from the measurement of the Fermi edge of Pd metal.

Photoelectrons were deaccelerated in front of the entrance to the energy analyzer, so that photoelectrons excited with radiation at different energies pass the energy analyzer with nearly the same kinetic energies. The retarding field, provided with two conical electrodes, deviated from an ideal spherical field, and this could distort the energy distribution curve. We measured the valence-band spectra of Au with various retarding voltages to estimate the amounts of the distortions of the energy distribution curves. The distortion was found to be small in the energy range, in which we are interested. Thus, we neglected the effect of the distortion.

III. RESULTS

The typical examples of the valence-state spectra as observed are shown in Fig. 1 for the four chlorides. The excitation energy is 76 eV. The ordinate represents output counts per channel N_{obs}. No attempt was made to correct the charging up of samples during measurements. Thus, the absolute value of binding energy can not be determined. The abscissa represents the binding energy in a relative scale. The four spectra are placed in a manner that the first peak of each spectrum occurs at nearly the same position. Peaks or fine structures found in the spectra are indicated by arrows and referred to as A through E. In $FeCl_2$, three peaks are clearly resolved. Such clearly resolved peaks are not found in the XPS spectrum of $FeCl_2$ as observed[6]; their existence is predicted from the profile of the deconvoluted spectrum. A similar situation is found in the case of $MnCl_2$. Two definite peaks occur in the spectrum of $MnCl_2$ in Fig. 1. In the XPS spectrum as observed,[6] the peak A at the low-binding-energy onset of the spectrum is not resolved well. These features are due to the better instrumental resolution in the present case.

Figures 2–5 show the energy distribution of valence-state photoelectrons for $NiCl_2$, $CoCl_2$, $FeCl_2$, and $MnCl_2$, respectively. Abscissas represent the relative scale of binding energy as in Fig. 1. Ordinates give the output counts divided by the voltage across the analyzer electrodes, N_{obs}/V_p. The backgrounds due to inelastically scattered electrons were subtracted under the assumption that they have a profile of linear dependence on binding energy. This assumption does not yield any noticeable errors in the following discussion, since the background intensities are weak. Three curves in each figure show the spectra obtained by excitation at 76, 61, and 40 eV from the top to the bottom. For $CoCl_2$, the spectra by excitation at 76 and 40 eV are shown.

Figures 2–5 indicate that the spectral profile

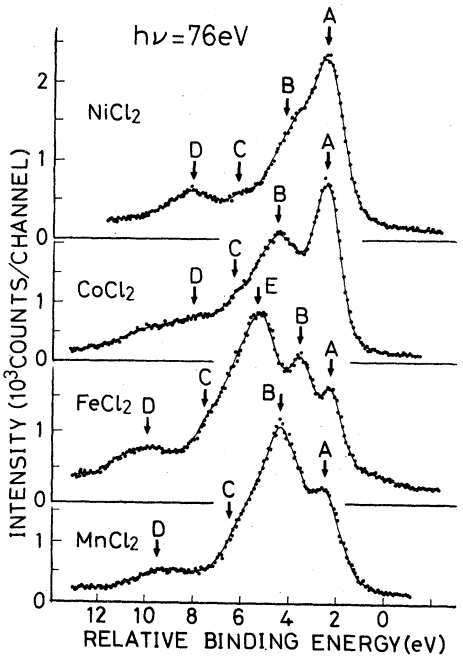

FIG. 1. Valence-state photoemission spectra of $NiCl_2$, $CoCl_2$, $FeCl_2$, and $MnCl_2$ as observed. Excitation energy is 76 eV. Structures in the spectra are indicated by arrows and labeled with capital letters A–E.

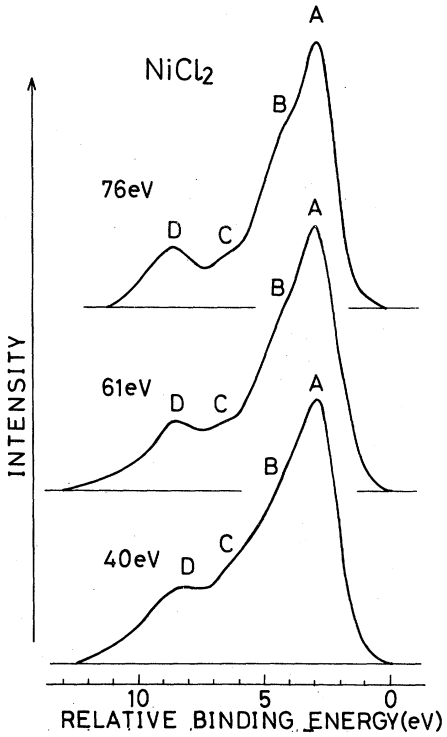

FIG. 2. Valence-state photoemission spectra of $NiCl_2$ excited with radiation at 76, 61, and 40 eV. Linear backgrounds are subtracted after the spectra as observed are multiplied by V_p at each measured point.

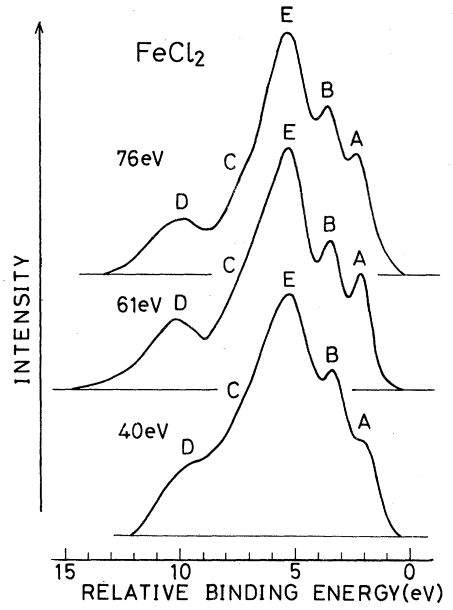

FIG. 4. Valence-state photoemission spectra of $FeCl_2$ excited with radiation at 76, 61, and 40 eV. Linear backgrounds are subtracted after the spectra as observed are multiplied by V_p at each measured point.

does not change with excitation energy: For one material, all fine structures are common in the spectra obtained by excitation at different energies. The relative intensities of various peaks estimated from the ratios of peak heights are tabulated in Table I. Structures discernible only as

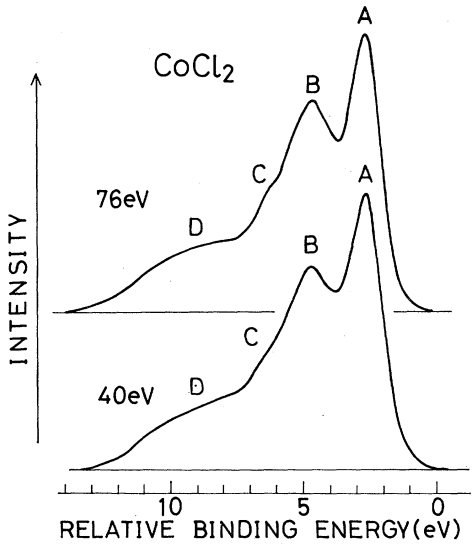

FIG. 3. Valence-state photoemission spectra of $CoCl_2$ excited with radiation at 76 and 40 eV. Linear backgrounds are subtracted after the spectra as observed are multiplied by V_p at each measured point.

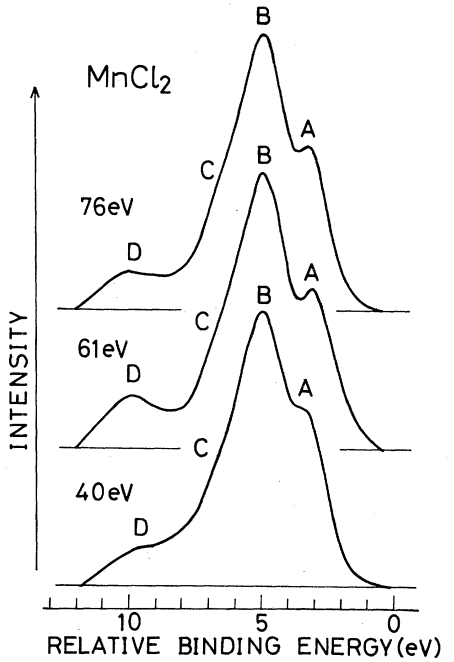

FIG. 5. Valence-state photoemission spectra of $MnCl_2$ excited with radiation at 76, 61, and 40 eV. Linear backgrounds are subtracted after the spectra as observed are multiplied by V_p at each measured point.

TABLE I. Relative peak heights for different excitation energies.

Sample	Excitation energy (eV)	Peak A	B	E	D
$NiCl_2$	76	1			0.23
	61	1			0.25
	40	1			0.27
$CoCl_2$	76	1	0.76		0.24
	40	1	0.74		0.22
$FeCl_2$	76	1	1.4	2.1	0.48
	61	1	1.3	1.9	0.58
	40	1	1.6	2.2	0.59
$MnCl_2$	76	1	1.5		0.24
	61	1	1.6		0.31
	40	1	1.4		0.22

small humps, like *C* in all materials and *B* in $NiCl_2$, are not given in Table I. The estimation of the intensities in Table I involves an error of about 10% including the error arising from the neglect of the correction for the modification of the spectrum due to the distortion of the retarding field. If such an error is taken into account, Table I appears to indicate that relative intensities of various peaks change only slightly among the spectra with three different excitation energies. Along with no dependence of the spectral profile on excitation energy, it is concluded that the spectrum itself depends on excitation energy only slightly in the energy region employed here.

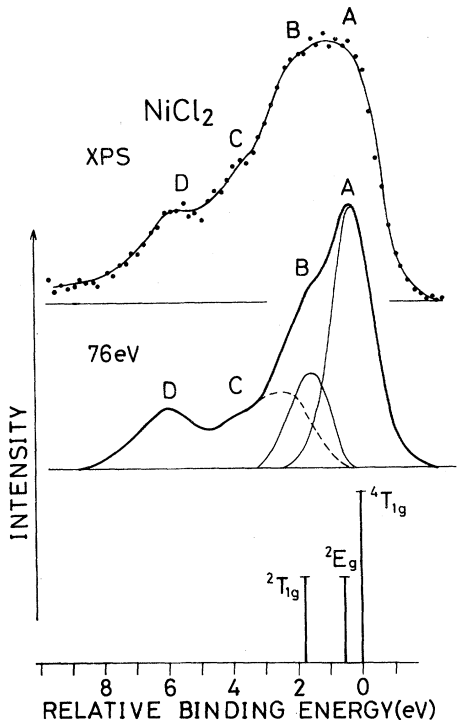

FIG. 6. XPS spectrum compared with the EUPS spectrum excited with radiation at 76 eV for $NiCl_2$. The distribution of the 3*d* levels of a Ni^{2+} ion calculated by a simple ligand-field treatment is shown at the bottom. Thin lines under the EUPS spectrum show the component bands of the 3*d* spectrum. Broken line shows the contribution of the 3*p* state of chlorine.

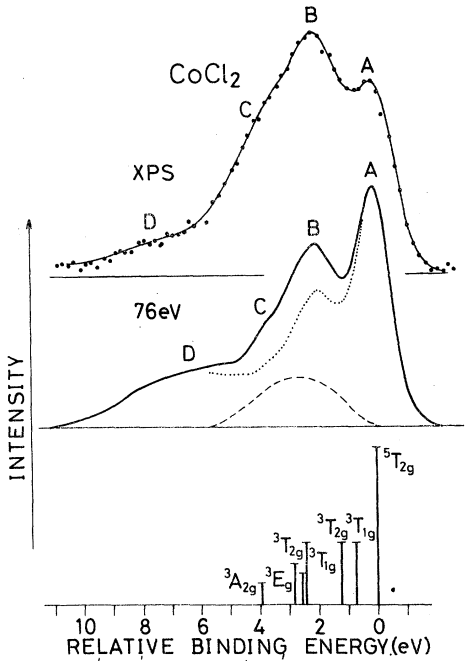

FIG. 7. XPS spectrum compared with the EUPS spectrum excited with radiation at 76 eV for $CoCl_2$. The distribution of 3*d* levels of a Co^{2+} ion calculated by a simple ligand-field treatment is shown at the bottom. Broken line under the EUPS spectrum shows the contribution of the 3*p* state of chlorine. The remaining 3*d* band of Co^{2+} is shown by dotted line.

Figures 6–9 show the comparison of the EUPS spectra obtained by 76-eV excitation with the XPS spectra obtained by Mg-$K\alpha$ excitation. The EUPS spectra are the same as those shown in Figs. 2–5. At the bottom of each figure, the line distribution of the 3*d* levels of the transition-metal ion predicted by a simple ligand-field treatment is shown for comparison. Under each EUPS spectrum, the spectrum of the 3*p* electrons of chlorine obtained by comparison with the XPS spectrum is shown by broken line. Curves drawn by thin lines under the EUPS spectrum show the component bands of the spectrum of 3*d* electrons of a transition-metal ion. The procedure to derive the broken and thin curves is described in Sec. IV along with the explanation of the curves. The XPS spectra were obtained by Sakisaka *et al.*[6] Figures 6–9 seem to indicate that the gross features of the EUPS spectra resemble those of the XPS spectra. For this reason,

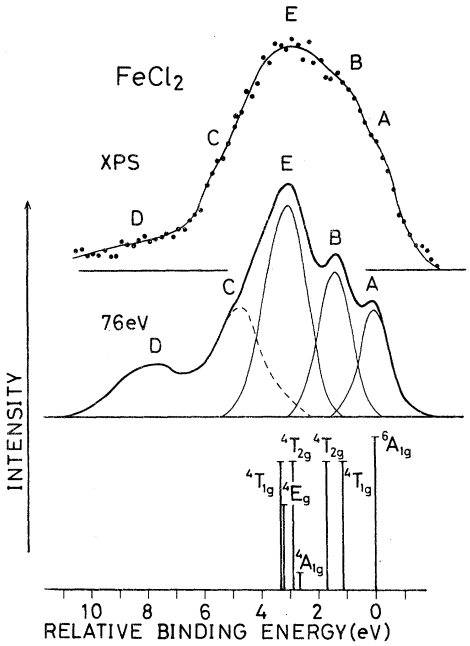

FIG. 8. XPS spectrum compared with the EUPS spectrum excited with radiation at 76 eV for $FeCl_2$. The distribution of the 3*d* levels of an Fe^{2+} ion calculated by a simple ligand-field treatment is shown at the bottom. Thin lines under the EUPS spectrum show the component bands of the 3*d* spectrum. Broken line shows the contribution of the 3*p* state of chlorine.

the structures in the XPS spectra are labelled with the same capital letters as those in the EUPS spectra according to the correspondence of the structures between both spectra. However, one clear difference between the EUPS and XPS spectra is found: The relative intensities in the regions 3–5 eV above the low-binding-energy edge are reduced in the EUPS spectra. For instance, the relative intensities of humps *B* and *C* are considerably decreased in the EUPS spectrum of $NiCl_2$. In $CoCl_2$, the intensity of peak *A* is larger than that of peak *B*, while this intensity relation is reversed in the case of XPS. Hump *C* is weak in the EUPS spectrum of $MnCl_2$. In addition to the reduction of the relative intensity of this hump, the intensity of peak *B*, is reduced as compared to peak *A*. In the case of $FeCl_2$, the situation is different. Figure 8 shows that the spectral intensity distribution of the XPS spectrum is nearly the same as that of the EUPS spectrum, except that the resolution is better in the latter. This will be interpreted as the contribution of the 3*p* electrons of chlorine being as small as in the case of XPS for $FeCl_2$.

IV. DISCUSSION

It is obvious that the valence state of a transition-metal chloride is formed by 3*d* electrons of the transition metal and 3*p* electrons of chlorine. Among the fine structures occurring in the photoelectron spectra presented here, we assume that humps *C* arise from Cl 2*p* electrons. This assumption reasonably explained the XPS spectra of these chlorides.[6,7] The similar assumption on the contribution of *p* electrons of anions has been shown to explain the valence-state photoelectron spectra of the oxides of transition metals.[7,8]

In the EUPS spectra of transition-metal halides, only slight dependence of the spectra on excitation energy is found at energies 76, 61, and 40 eV. We suppose that the difference of excitation energy is unimportant in the photoemission process in this energy region. The partial density of states is important there.[9] Little dependence of the spectrum on excitation energy indicates that the energy dependence of the ratio σ_{3p}/σ_{3d} of the ionization cross section between a 3*d* electron of a transition-metal ion and a 3*p* electron of chlorine does not vary much with excitation energy. Perhaps σ_{3p}/σ_{3d} is small, and the contribution of the 3*d* electron of transition-metal ions is conspicuous in this energy region. This interpretation will also explain the clear difference between the EUPS and XPS spectra, i.e., the reduction of the relative intensity of humps *C* in the EUPS spectra. The re-

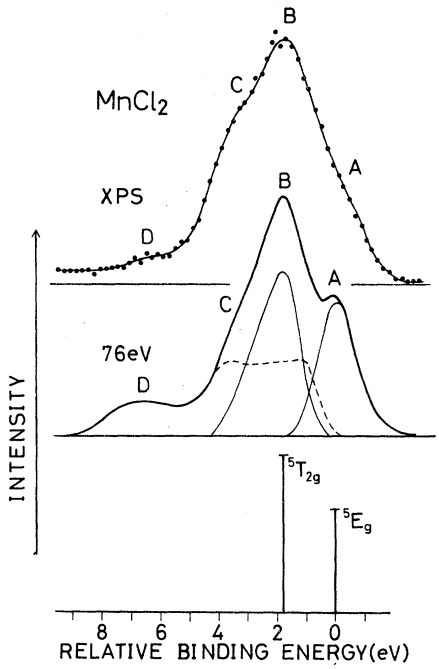

FIG. 9. XPS spectrum compared with EUPS spectrum excited with radiation at 76 eV for $MnCl_2$. The distribution of 3*d* levels of an Mn^{2+} ion calculated by a simple ligand-field treatment is shown at the bottom. Thin lines under the EUPS spectrum show the component bands of the 3*d* spectrum. Broken line shows the contribution of the 3*p* state of chlorine.

duction of the relative intensity of peak B relative to peak A in the EUPS spectrum of $CoCl_2$ as compared to the XPS spectrum may be explained in a similar way. The overlap of hump C and peak B is large in $CoCl_2$, and the reduction in the intensity of hump C leads to the apparent reduction in the intensity of peak B. In the previous interpretation of the XPS spectrum of $NiCl_2$, the broadness of the main band was attributed only to a small value of Dq.[6,7] The contribution of the $3p$ electrons of chlorine is as important as the small value of Dq. The reduction of the relative intensity of peak B in $MnCl_2$ is a little puzzling. One possible explanation is that the $3p$ electrons of chlorine have the nonvanishing density of states contributing to the spectrum in the region of peak B; the reduction in the intensity of peak B is due to the reduced relative contribution of the $3p$ electrons of chlorine, as in the case of $CoCl_2$.

Humps C remain undiminished in the EUPS spectra, though they are weak. Therefore, the ionization cross section of a $3p$ electron of chlorine still has a nonvanishing value in the extreme-ultraviolet region. According to the measurements on transition-metal oxides by Eastman and Freeouf,[8] the relative contribution of the $3d$ electrons of transition metals seems to increase monotonically with the energy of exciting radiation, and the contribution of the $2p$ electrons of oxygen is very small in the case of XPS. The small contribution of the $2p$ electrons of oxygen was also found in the case of XPS of ReO_3.[10] It appears that the relative contribution of the $3d$ electrons transition-metal ions is largest in the extreme-ultraviolet region in the case of the chlorides. If we assume that the chlorine $3p$ state does not have energy levels in the regions of peaks A, the chlorine $3p$ spectra can be obtained by subtracting the EUPS spectra from the XPS spectra. There, the intensities of both spectra should be normalized at peaks A prior to the subtraction. Similar procedures to separate the contribution of the $3d$ electrons of the metal ion from that of the p electrons of the ligand anion were first developed by Eastman and Freeouf[8] and Goldmann *et al.*[11] In Figs. 6–9, the $3p$ bands of chlorine estimated in this manner are shown by broken lines. In the case of $FeCl_2$, the procedure described above is not applicable, since the spectral intensity distribution is nearly the same in XPS and EUPS. Thus, we decomposed the three definite peaks in the EUPS spectrum into components under the assumption that each peak arises from a single band with a symmetrical line shape. The band remaining after subtracting the $3d$ bands thus obtained is supposed to give the contribution of the $3p$ levels of chlorine, and it is shown by broken line in Fig. 8. The bands obtained after subtraction of broken curves from the EUPS spectra in Figs. 6–9 represent the contributions due to the $3d$ electrons of transition-metal ions. The bands are tentatively decomposed into components under the assumption that the A band has a symmetrical line shape. The components are shown by thin lines in Figs. 6–9. The relative intensities of the components estimated from the ratios of the areas under thin curves in the figures are given in Table II along with the expectations from ligand-field theory.

The major features of the EUPS spectra obtained here are determined by the spectral distribution of the $3d$ levels of the transition metals. A transition-metal ion is surrounded by neighboring ligand anions octahedrally. The energy levels may be approximated by those of a molecular ion MCl_6^{4-}; M stands for the transition metal. In the first approximation, the spectral distribution of the $3d$ levels of transition-metal ions may be obtained by ligand-field theory. The spectra may

TABLE II. Relative integrated intensities of component bands of transition-metal $3d$ photoelectrons and corresponding predictions from ligand-field theory.

Sample	$NiCl_2$		$CoCl_2$		$FeCl_2$			$MnCl_2$	
Peak	A	B	A	B	A	B	E	A	B
Relative intensity observed	1	0.36	1	0.85	1	1.5	2.7	1	1.4
Component level	$^4T_{1g}{}^2E_g$	$^2T_{1g}$	$^5T_{2g}{}^3T_{1g}{}^3T_{2g}$	$^3T_{1g}{}^3T_{2g}{}^3E_g{}^3A_{2g}$	$^6A_{1g}$	$^4T_{1g}{}^4T_{2g}$	$^4A_{1g}{}^4T_{2g}{}^4E_g{}^4T_{1g}$	^5E_g	$^5T_{2g}$
Relative transition probability	2 1	1	15 6 6	6 3 4 2	18	15 15	2 15 10 15	2	3
Relative intensity expected	1	0.33			1	1.7	2.3	1	1.5

reflect the energy levels of the state with the $3d^{N-1}$ configuration in the final state; N is the number of $3d$ electrons in a metal ion in the initial state. On the basis of the strong-field scheme,[4] it is not difficult to find what kind of energy terms occur in the present problem, provided that the configuration mixing, which may be important for the electron-correlation effects in the final state, is neglected to the first approximation. The multiplet levels of the ground states are $^3A_{2g}$, $^4T_{1g}$, $^5T_{2g}$, and $^6A_{1g}$, for $NiCl_2$, $CoCl_2$, $FeCl_2$, and $MnCl_2$, respectively.[4,8] The levels attainable from these levels by photoejection of electrons are tabulated in Table II. The transition probabilities to the levels in the final state are given in terms of the Clebsch-Gordan coefficients, $6j$ symbols, the coefficients of fractional parentage, and the reduced transition-matrix element of a single $3d$ electron. The derivation of the formula of the transition probability is rather straightforward and has first been carried out by Satoko and Sugano.[12,13] The relative values of the transition probabilities are given in Table II. There, the assumption is made that the reduced transition-matrix element is the same for the e_g and t_{2g} electrons.

The energy distributions of the component levels given in Table II are predicted by the help of the energy-level diagram obtained by Tanabe and Sugano.[14] Good agreement between the observed spectra and the line distributions of the component levels predicted is obtained if we choose Racah parameters and crystal-field parameters as follows: $B = 0.094$ eV, $\gamma (\equiv C/B) = 4.63$, and $10Dq = 1.5$ eV for $NiCl_2$; $B = 0.098$ eV, $\gamma = 4.81$, and $10Dq = 2.0$ eV for $CoCl_2$; $B = 0.082$ eV, $\gamma = 4.48$, and $10Dq = 1.8$ eV for $FeCl_2$; $10Dq = 1.7$ eV for $MnCl_2$. The line distributions of the component levels corresponding to these parameters are shown in Figs. 6–9 for the comparison with the observed spectra. The vertical bars showing each component line are drawn in a manner such that their lengths are proportional to the relative transition probability in Table II. B can not be evaluated from the experimental data obtained here for $MnCl_2$, because only two lines exist. In $CoCl_2$, the overlap of the Cl^- $3p$ band and the Co^{2+} $3d$ bands is large, and the estimation of the Cl^- $3p$ band includes ambiguity. The locations of the $^3T_{2g}$ and $^3T_{1g}$ lines with high energy are not known for all values of Dq/B. The line distribution shown in Fig. 7 and the parameters described above are obtained as the best-fit case here. The agreement with the observed spectrum is still fair qualitatively, except that the locations of first three lines are too widely spread to explain the width of the observed first peak. Asada *et al.*[15] analyzed the satellites of core level lines in x-ray photoemission and x-ray emission. They obtained a value of 2.0 eV for $10Dq$ of $NiCl_2$. Since the detailed processes involved in the present experiment are different from those of core excitation, Dq may be different.

A remarkable feature of the comparison of the above results of ligand-field theory with the observed spectra is the good agreement of line intensities between the experimental results and theory. In $NiCl_2$, for example, the $^4T_{1g}$ line and the ^2E_g line appear to bunch together to form peak A, and the $^2T_{1g}$ line forms peak B. According to this assignment, the ratio of the integrated intensity of peak A to that of peak B is expected to be $3:1 \simeq 1:0.33$ as shown in Table II. The observed ratio between the integrated intensities of the component bands shown by thin lines in Fig. 6 is $1:0.36$, in good agreement with the expectation. In $FeCl_2$, $3d$ electrons of an Fe^{2+} ion produce three bands. As is obvious in Fig. 8, peak A is ascribed to the $^6A_{1g}$ line, peak B to a bunch of the $^4T_{1g}$ and $^4T_{2g}$ lines, peak E to a bunch of the $^4T_{1g}$, $^4T_{2g}$, ^4E_g, and $^4T_{1g}$ lines. The expected ratio of intensity between three groups of lines is $18:30:42 \simeq 1:1.7:2.3$, where the observed ratio of the integrated intensities of the component bands is $1:1.5:2.7$. For $MnCl_2$, the theory predicts only two lines, ^5E_g and $^5T_{2g}$, with intensity ratio $2:3$. Two peaks are clearly seen in the spectra in Fig. 5. The ratio between the integrated intensities of the component bands in Fig. 9 is $1:1.4$. The $3p$ band of chlorine in $MnCl_2$ shown in Fig. 9 has a rather peculiar shape. This might be a result of the assumption that the contribution of the $3p$ electrons of chlorine vanishes in the region of peak A. If the A and B peaks in the EUPS spectrum are decomposed in the same way as in Fig. 8 for $FeCl_2$, the result gives a narrower and well-shaped curve for the $3p$ band of chlorine. In this case, a value of $1:1.6$ is obtained as the ratio of the integrated intensity between the A and B peaks. However, such a decomposition can not explain the reduction in the relative intensity of peak B in the EUPS spectrum as compared to the XPS spectrum. In any case, the ratio does not seem to deviate much from $1:1.5$.

The good agreement of the results of the simple ligand-field treatment with the experimental results presented here includes a slight accidental part, since the decomposition of the spectrum such as shown in Figs. 6–9 always contains some ambiguity. In the sense of the molecular-orbital approach, the reduced transition-matrix element may be different for the e_g and t_{2g} orbitals owing to the different amount of the mixing of the chlorine $3p$ orbitals[16] as well as the different values of the normalization factors. The configuration interaction should alter the energy levels given by the simple ligand-field treatment. The good agreement of the line distribution given by the

simple theory with the experimental results appears to suggest that the effects of the mixing of the $3p$ state of chlorine and of the electron correlation in the $3d$ state of the transition-metal ion on energy separations among various lines may be renormalized into the Racah parameters B and C and the crystal-field parameter Dq through scaling. At this stage, it should be noted that a molecular-orbital calculation based on the self-consistent-field–$X\alpha$ method has been reported by Johnson *et al.*[17] Their result seems to have a good correspondence with the experimental result on NiO as far as the energy positions of levels are concerned. However, the Hamiltonian is diagonalized with respect to S_z in this method. It appears that diagonalization of Hamiltonian as to S^2 may also be necessary to get the agreement with the experimental results concerning the spectral intensity distribution.

Peak D is found in all the chlorides measured here. Wertheim *et al.*[7] and Eastman and Freeouf[8] attributed similar weak peaks found in the oxides to multielectron satellites. We attribute peak D to such a multielectron process. In $MnCl_2$, two component lines of $3d$ electrons obtained by the decomposition have a half-width of about 1.7 eV. This value is three times larger than the width of the instrumental resolution. Therefore, each component line of the $3d$ levels has an appreciable intrinsic width. Satoko and Sagano[18] suggested the possibility that the width may be caused by mobile $3d$ holes produced by photoejection of electrons. The electron-phonon interaction may also cause the line broadening in a polarizable medium like the materials used here. Recently, Citrin *et al.*[19] showed in their XPS experiment that core level lines in alkali halides are broadened by the significant contribution of phonons. We can not rule out the possibility of phonon-induced broadening, since the lattice relaxation accompanying photoemission is a kind of many phonon process.

ACKNOWLEDGMENTS

The authors appreciate Professor S. Sugano and Dr. C. Satoko for many valuable suggestions and stimulating discussions. One of the authors (T. I.) wishes to thank Professor A. Yanasa for helpful discussions.

---

*Research supported by the Grant-in-Aid from the Ministry of Education and by the Mitsubishi Scientific Foundation.

†Present address: Faculty of Education, Gumma University, Maebashi.

‡Permanent address: Dept. of Physics, Tohoku University, Sendai.

§Permanent address: Dept. of Physics, Kyoto University, Kyoto.

[1]R. S. Knox, *Theory of Excitons* (Academic, New York, 1963).

[2]F. C. Brown, *Solid State Physics*, edited by H. Ehrenreich, F. Seitz, and D. Turnbull (Academic, New York, 1974), Vol. 29, p. 1.

[3]D. Adler, *Solid State Physics*, edited by F. Seitz, D. Turnbull, and H. Ehrenreich (Academic, New York, 1968), Vol. 21, p. 1.

[4]S. Sugano, Y. Tanabe, and H. Kamimura, *Multiplets of Transition-Metal Ions in Crystals* (Academic, New York, 1970).

[5]T. Sagawa, R. Kato, S. Sato, M. Watanabe, T. Ishii, I. Nagakura, S. Kono, and S. Suzuki, J. Electron Spect. Rel. Phenom. 5, 551 (1974).

[6]Y. Sakisaka, T. Ishii, and T. Sagawa, J. Phys. Soc. Jpn. 36, 1365 (1974).

[7]G. K. Wertheim, H. J. Guggenheim, and S. Hüfner, Phys. Rev. Lett. 30, 1050 (1973).

[8]D. E. Eastman and J. L. Freeouf, Phys. Rev. Lett. 34, 395 (1975).

[9]P. J. Feibelman, and D. E. Eastman, Phys. Rev. B 10, 4932 (1974).

[10]G. K. Wertheim, L. F. Mattheiss, and M. Campagna, Phys. Rev. Lett. 32, 997 (1974).

[11]A. Goldmann, J. Tejeda, N. J. Shevchik, and M. Cardona, Phys. Rev. B 10, 4388 (1974).

[12]C. Satoko, thesis (University of Tokyo, 1974) 2, 168 (1974).

[13]C. Satoko, thesis (University of Tokyo, 1974) (unpublished).

[14]Y. Tanabe and S. Sugano, J. Phys. Soc. Jpn. 9, 766 (1954).

[15]S. Asada, C. Satoko, and S. Sugano, J. Phys. Soc. Jpn. 38, 855 (1975).

[16]One could explain the reduced intensity of the E_g peak in XPS in terms of the reduced contribution of the $3p$ electrons of chlorine in the XPS case, since the mixing of the $3p$ state of chlorine is larger in the bonding e_g orbital. If this were correct, one would not be able to explain the reduction of the hump on the high-binding-energy side of the highest peak arising from the $3p$ level of chlorine.

[17]K. H. Johnson, R. P. Messmer, and J. W. D. Connolly, Solid State Commun. 12, 313 (1973).

[18]C. Satoko and S. Sugano, Buturi 29, 1026 (1974) (in Japanese).

[19]P. H. Citrin, P. Eisenberger, and D. R. Hamann, Phys. Rev. Lett. 33, 965 (1974).